Heliyon 8 (2022) e10625

Contents lists available at ScienceDirect

Heliyon

journal homepage: www.cell.com/heliyon

Research article

The palladium-based complexes bearing 1,3-dibenzylbenzimidazolium with morpholine, triphenylphosphine, and pyridine derivate ligands: synthesis, characterization, structure and enzyme inhibitions

Aydın Aktaş [a], Gül Yakalı [b], Yeliz Demir [c], İlhami Gülçin [d,*], Muhittin Aygün [e], Yetkin Gök [f]

[a] Inonu University, Vocational School of Health Service, 44280, Malatya, Turkey
[b] Department of Engineering Sciences, Faculty of Engineering, Izmir Katip Celebi University, 35620, Izmir, Turkey
[c] Department of Pharmacy Services, Nihat Delibalta Göle Vocational High School, Ardahan University, 75000, Ardahan, Turkey
[d] Atatürk University, Faculty of Science, Department of Chemistry, 25240, Erzurum, Turkey
[e] Department of Physics, Faculty of Arts and Sciences, Dokuz Eylül University, 35150, Izmir, Turkey
[f] Department of Chemistry, Faculty of Science and Arts, Inonu University, 44280, Malatya, Turkey

ARTICLE INFO

Keywords:
Acetylcholinesterase
Bio-catalysis
NHC
Palladium complexes
PEPPSI
Single crystal
Carbonic anhydrases

ABSTRACT

The palladium-based complexes bearing *N*-heterocyclic carbene (NHC) ligand have long attracted attention as active catalysts for many catalytic reactions. Recently, the biological activities of these complexes, which are stable to air and moisture, have also been wondered. With the aim, we report the synthesis of a series of (NHC) $Pd(Br_2)(L)$ complexes (NHC: 1,3-dibenzylbenzimidazolium, L: morpholine, triphenylphosphine, pyridine, 3-chloropyridine, and 2-aminopyridine). All complexes were characterized by NMR (^1H and ^{13}C), FTIR spectroscopic and elemental analysis techniques. In addition, the single crystal structures of the complex **3**, **4**, and **6** were determined through single crystal x-ray crystallographic method. Furthermore, the carbonic anhydrase I and II isoenzymes (hCAs) and acetylcholinesterase (AChE) inhibition effects of these palladium-based complexes bearing NHC ligand were investigated. They showed highly potent inhibition effect with K_i values are between 10.06 ± 1.49–68.56 ± 11.53 nM for hCA I isoenzyme, 7.74 ± 0.66 to 49.39 ± 6.50 nM for hCA II isoenzyme and 22.83 ± 3.21 to 64.09 ± 9.05 nM for AChE enzyme.

1. Introduction

N-heterocyclic carbene (NHC) is important supporting ligands [1] with their innovative biological effects [2]. The steric and electronic properties of NHC have contributed to their being at the forefront of many advances [3]. The NHC and phosphine ligands have played a crucial role to develop organometallic chemistry. These ligand classes, combining two-electron, neutral, and σ-donor have enriched the applications of transition metal complexes [4]. Diverse approaches have been made to add a phosphine group to the NHC skeleton in the synthesis of organometallic compounds, and metalation has been successfully accomplished through both functionalities [5]. The halide ligand and phosphine molecule used in such complexes are thought to hydrolyze and facilitate the *in vitro* stabilization of complex ions formed by the metal reduction in the metal's coordination sphere [6]. Phosphine-based ligands have widespread pharmacological applications, including antibacterial antioxidant, anticarcinogenic, antiviral, antifungal, and antitumor [7]. It has been recorded that especially phosphine-based nickel (II) and palladium (II) complexes have important bioactivities [8]. These metals-based complexes are used as valuable anticancer drugs due to their effects such as inhibiting cell division and controlling gene expression. The problem with these complexes is that they decompose into highly reactive species in solution, so do not reach their pharmacological targets such as DNA. However, this can be avoided by stabilizing the Nickel (II) and palladium (II) complexes by bulky ligands such as triphenylphosphine [6, 9].

In 2006, Organ et al reported a class of precatalysts based on Pd(II) containing pyridine derived ligands [10]. The complexes consist of one NHC, two anions (usually Cl or Br), and stabilizing throw-away pyridine derivative ligands [11, 12, 13]. Recently, new works have been reported on the antimicrobial, anticancer, antileishmanial, antitoxoplasmal, and enzyme inhibition activities of the PEPPSI type Pd(II)NHC complexes [14, 15]. In this work, pyridine, 3-chloropyridine, and 2-aminopyridine ligands were used as pyridine derivatives. Numerous *in vitro* studies

* Corresponding author.
E-mail addresses: igulcin@atauni.edu.tr, igulcin@yahoo.com (İ. Gülçin).

https://doi.org/10.1016/j.heliyon.2022.e10625
Received 17 May 2022; Received in revised form 17 July 2022; Accepted 8 September 2022

Table 1. Crystallographic details for the complexes 3, 4 and 6.

Name	Complex 3	Complex 4	Complex 6
Empirical formula	$C_{26}H_{22}Br_2ClN_3Pd$	$C_{26}H_{24}$ Br_2N_4Pd	$C_{25}H_{27}$ Br_2N_3OPd
Formula weight	678.13	658.71	651.71
Temperature (K)	293 (2)	293 (2)	293 (2)
Crystal system	Triclinic	Monoclinic	monoclinic
Space group	P-1	$P2_1/n$	I2/a
Unit cell dimensions a (Å)	10.5516 (11)	11.7062 (7)	18.9096 (6)
b (Å)	12.5449 (11)	7.5947 (4)	10.1803 (4)
c (Å)	19.2857 (17)	28.2645 (13)	26.8057 (8)
α (°)	97.937 (7)	90	90
β (°)	91.737 (8)	93.403 (5)	106.021 (4)
γ (°)	92.095 (8)	90	90
Volume/(Å^3)	2525.1 (4)	2508.4 (2)	4959.8 (3)
Z	4	4	8
D_{calc} (g/cm^{-3})	1.784	1.744	1.746
Absorption coefficient (mm^{-1})	4.025	3.947	3.993
F (000)	1328.0	1296.0	2576.0
Crystal size (mm)	0.33 × 0.3 × 0.23	0.479 × 0.263 × 0.206	0.394 × 0.324 × 0.248
h ranges	−11→12	−13→14	−22→22
k range	−14→14	−8→9	−12→10
l range	−18→22	−34→17	−32→18
Reflections collected/unique	11563/11563	7891/4708	9916/4693
Data/restrains/parameters	11563/27/596	4708/12/298	4693/0/289
Goodness of fit on F^2	1.063	1.033	1.028
Final *R* indices [$I > 2\sigma(I)$]	$R_1 = 0.0745$ $wR_2 = 0.1619$	$R_1 = 0.0382$ $wR_2 = 0.0824$	$R_1 = 0.0322$ $wR_2 = 0.0674$
R indices (all data)	$R_1 = 0.1387$ $wR_2 = 0.1968$	$R_1 = 0.0592$ $wR_2 = 0.0909$	$R_1 = 0.0491$ $wR_2 = 0.0737$
Largest difference peak and hole (e Å^{-3})	1.50/−0.87	1.03/−0.50	0.29/−0.67

have been reported in the literature regarding pyridine-based compounds as active enzyme inhibitors [16, 17, 18].

Carbonic anhydrase (CA) is a metalloenzymes group that participate in various physiologic and biochemical processes including pH control of extra/intracellular spaces by catalytic reversible hydration conversion of H_2O and CO_2 to H^+ and HCO_3^- [19]. The CA family includes eight different and distinct species: α-, β-, γ-, δ-, ζ-, η-, θ-, and t-CAs. Also, 16 different α-CA isozymes were defined up to now [20]. Of these CAs I-III, and VII are cytosolic forms, CAs IX, IV, XII, and XIV are membrane bounded isozymes, CA V is mitochondrial form and CA VI is secreted isoenzyme [21]. CA inhibitors (CAIs) exhibit some biological activities associated with several common diseases including cancer, glaucoma, epilepsy, obesity and osteoporosis [22]. CAs I and II isozymes are the most studied and well-known isoenzymes [23]. CA I is expressed in the gastrointestinal tract and erythrocytes. On the other hand, CA II is expressed in most of tissues including gastrointestinal tract, eye, bone osteoclasts, erythrocytes, testcle, kidney, lung and brain [24]. The reactions catalyzed by CA isoenzymes are vital in reactions and processes including ion transportation and fatty acid metabolism [25]. A high level of various CA isoforms in the body is linked to several disorders involving glaucoma, cancer, epilepsy and obesity [26, 27]. Recently, human CA Inhibitors (CAIs) have been effectively used to treat many diseases like epilepsy, intracranial hypertension, obesity and hypoxic tumors [28, 29]. CAIs were also used as important drugs for cerebral ischemia, neuropathic pain, arthritis and [30, 31].

The acetylcholinesterase (AChE) enzyme is an important target for Alzheimer's disease (AD) that has commonly affected the elderly people, especially after the age of sixty [32, 33]. The symptoms of AD appear gradually with age and over time. It makes the person unable to do their daily work and activities on their own [34, 35]. In the brain, the loss of neurotransmission and the deterioration of cholinergic neurons are the major causes of the decline in cognitive function in AD patients [36, 37]. One of the therapeutic approaches is AChE inhibitors (AChEIs) to limit the degradation of acetylcholine (ACh) [38]. AChEIs are able to increase the function of neural cells by increasing the ACh concentration. So, most studies have been focused on AChE inhibition and AChEIs for AD treatment [39, 40].

In the light of the above-mentioned information, the design and synthesis of more effective, new and potent CAs and AChEIs are of great importance. Recently, our research group has synthesized such complexes containing NHC ligands bearing different functional groups and determined the enzyme inhibitory effects of these complexes [12, 13, 14]. In this work, we aimed to examine the CAs and AChE inhibition activities of new (NHC)$PdBr_2$L complexes obtained by the coordination of various ligands without changing the NHC and halogen ligands coordinated to palladium metal. In this context, we synthesized (NHC)$PdBr_2$L complexes for identification of therapeutic potentials with the coordination of five different ligands (L: triphenylphosphine, morpholine, pyridine, 3-chloropyridine and 2-aminopyridine) with diverse electronic and structural properties apart from NHC and Br ligands. All synthesized complexes were characterized by NMR, FTIR methods, and elemental analysis technique. The molecular structures of three of these synthesized complexes were elucidated by the XRD method.

To our knowledge, the CAs and AChE inhibitory properties of palladium-based complexes bearing 1,3-dibenzylbenzimidazolium with morpholine, triphenylphosphine, and pyridine derivate ligands have not been reported up to date. Therefore, their CAs and AChE inhibition potentials were searched for the first time.

2. Experimental

2.1. General methods

All new complexes (**2–6**) containing 1,3-dibenzylbenzimidazolium ligand were synthesized by the standard Schlenk technique under an inert atmosphere. All reagents were obtained from Sigma-Aldrich, Merck, Isolab and Acros Chemical Co. The melting points were determined in glass capillaries under air with an Electrothermal-9200 apparatus. Also,

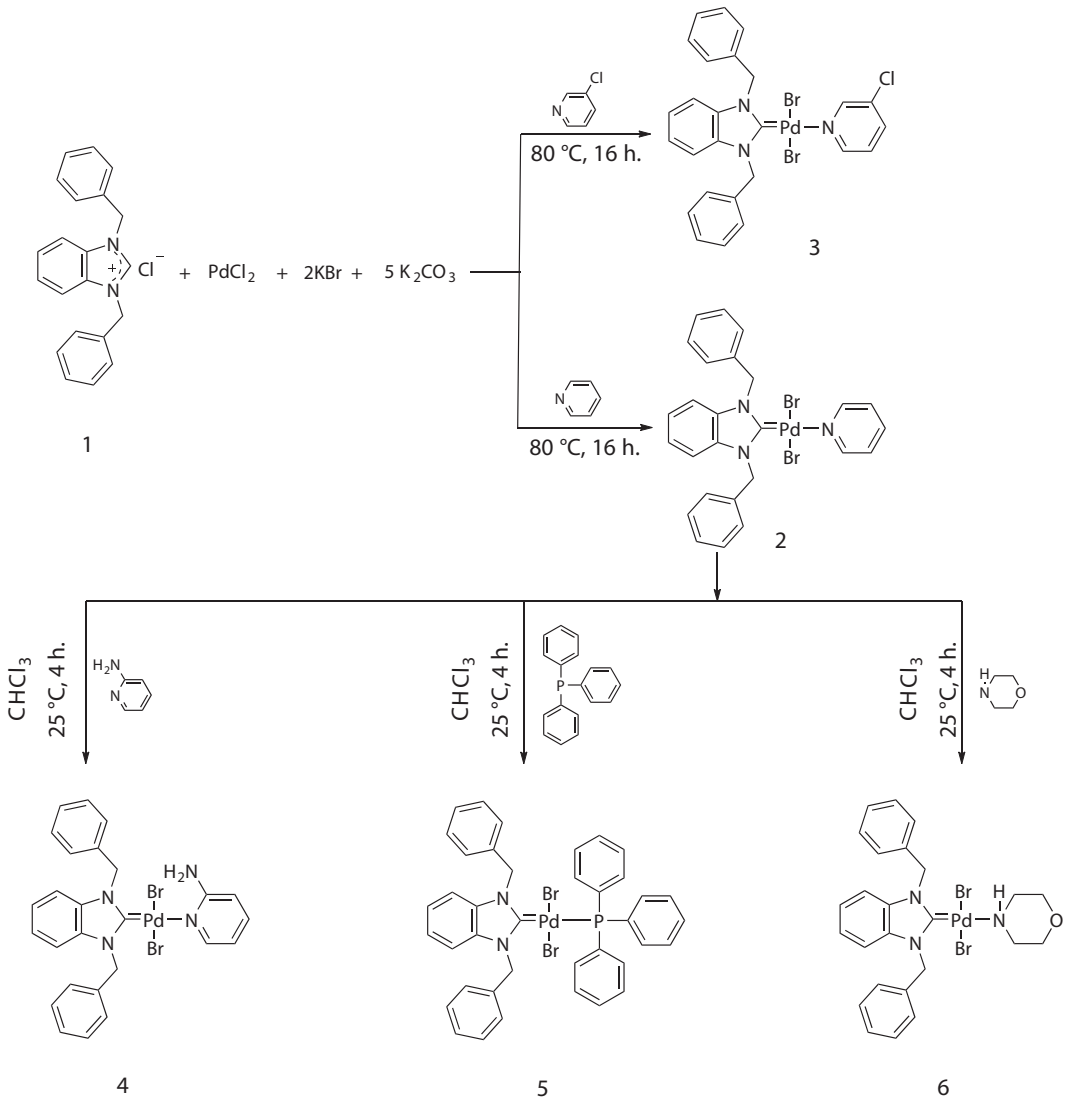

Scheme 1. Synthesis of the (NHC)$PdBr_2$L complexes (**2–6**).

FT-IR spectra were recorded in the range of 400–4000 cm^{-1} by PerkinElmer Spectrum 100 FTIR spectrometer. Proton (^1H) and Carbon (^{13}C) NMR spectra were recorded by a Bruker Avance III 400 MHz NMR spectrometer operating at 100 MHz (^{13}C), 400 MHz (^1H) in $CDCl_3$ with tetramethylsilane as an internal reference.

2.2. The blood sample supply

There is no clinical application in this study, so no animals or humans were used. Human erythrocytes used as carbonic anhydrase isoenzymes source in this study. Since expired waste blood was used in the study, permission was not obtained from our institution. Our institution has approved the use of expired blood samples in our experimental studies. The used human erythrocytes were the waste and expired blood that was procured from the Blood Center of Atatürk University Research Hospital. The blood donation was made by healthy volunteers on a national scale and an ethics committee certificate was not required.

2.3. Synthesis

2.3.1. Synthesis of the 1,3-dibenzylbenzimidazolium chloride, *1*

This known compound **1** [41] was prepared by mixing 1-benzylbenzimidazole (1.5 g, 7.2 mmol) and benzyl chloride (0.91 g, 7.2 mmol) in acetonitrile (5 mL) at 80 °C for 24 h. Yield: 86% (2.07 g); m.p.: 233–234 °C.

2.3.2. Synthesis of the dibromo[1,3-dibenzylbenzimidazol-2-ylidene] pyridinepalladium(II), *2*

This known complex **2** [42] was prepared by mixing 1,3-dibenzylbenzimidazolium chloride (200 mg, 0.6 mmol), palladium chloride (106 mg, 0.6 mmol), potassium bromide (143 mg, 1.2 mmol) and potassium carbonate (414 mg, 3 mmol) in pyridine (4 mL) at 80 °C for 16 h. Yield: 72% (278 mg); m.p.: 233–234 °C; $\nu_{(CN)}$: 1411 cm^{-1}.

2.3.3. Synthesis of the dibromo[1,3-dibenzylbenzimidazol-2-ylidene]-3-chloropyridinepalladium(II), *3*

The complex **3** was synthesized by the same method as complex **2**. But, 3-chloropyridine was used instead of pyridine as solvent and ligand. Yield: 68% (276 mg); m.p.: 226–227 °C; $\nu_{(CN)}$: 1411 cm^{-1}. Anal. Calc. for $C_{26}H_{22}Br_2ClN_3Pd$: C: 46.05; H: 3.27; N: 6.20. Found: C: 45.96; H: 3.33; N: 6.24. ^1H NMR (400 MHz, $CDCl_3$); δ 6.14 (d, 4H, J = 14.4 Hz, –NC***H***$_2C_6H_5$); 6.98–7.54 (m, 16H, Ar–***H*** and C***H***Py); 7.67 (m, 1H, C***H***Py); 8.88 (d, 1H, J = 5.4 Hz, C***H***Py); 8.98 (s, 1H, C***H***Py). ^{13}C NMR (100 MHz, $CDCl_3$) δ; 53.2 and 53.8 (-N***C***$H_2C_6H_5$); 111.5, 111.6, 123.3, 124.9, 128.0, 128.1, 128.3, 128.9, 132.6, 132.7, 134.7, 134.8, 134.9, 138.0 and 138.1 (Ar–***C***); 150.0, 150.6, 151.1 and 151.7 (***C***-Py); 163.3 (Pd-$C_{carbene}$).

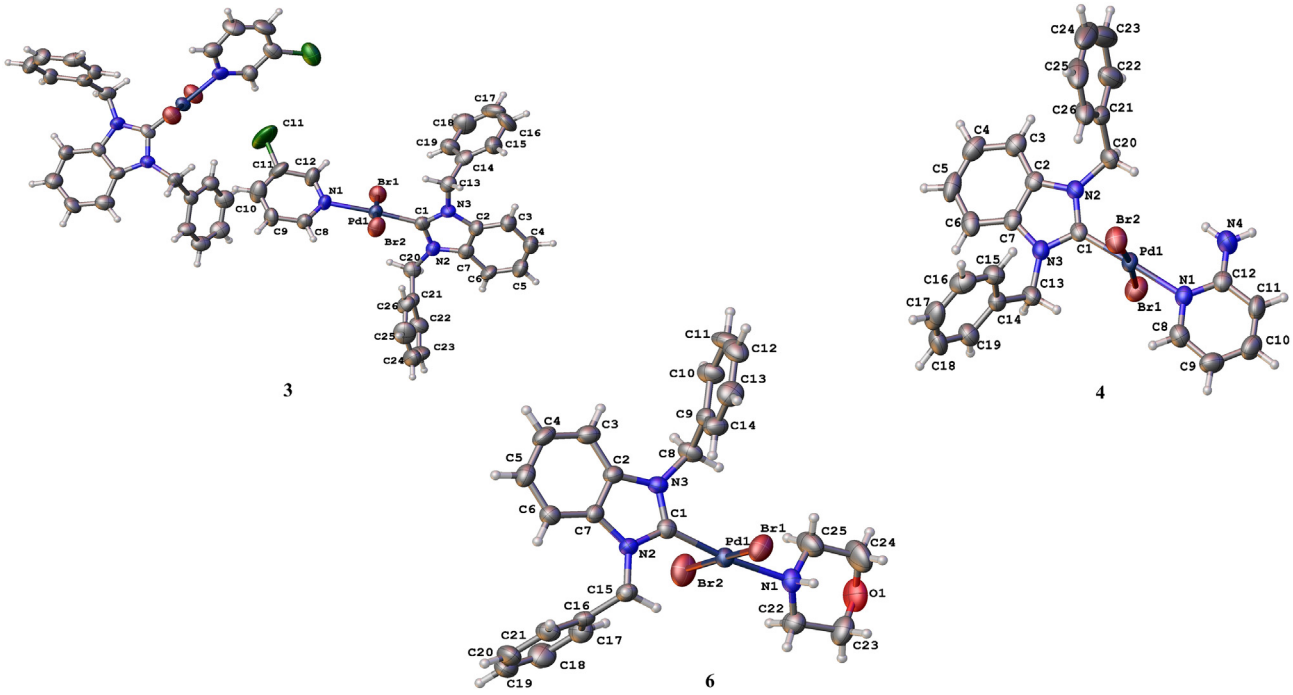

Figure 1. The molecular structure of the complexes **3**, **4**, and **6** showing the atom numbering scheme. Displacement ellipsoids are drawn at the 50% probability level and H atoms are shown as small spheres of arbitrary radii.

2.3.4. Synthesis of the dibromo[1,3-dibenzylbenzimidazol-2-ylidene]-2-aminopyridinepalladium(II), *4*

The complex **4** was prepared by mixing dibromo[1,3-dibenzylbenzimidazol-2-ylidene]pyridinepalladium(II) (129 mg, 0.2 mmol) and 2-aminopyridine (19 mg, 0.2 mmol) in chloroform (15 mL) at 25 °C for 6 h. Yield: 76% (100 mg); m.p.: 265–266 °C; $\nu_{(CN)}$: 1411 cm^{-1}; $\nu_{(N-H)}$: 3325 cm^{-1} and 3448 cm^{-1}. Anal. Calc. for $C_{26}H_{24}Br_2N_4Pd$: C: 47.41; H: 3.67; N: 8.51. Found: C: 47.55; H: 3.60; N: 8.46. ^{1}H NMR (400 MHz, $CDCl_3$); δ 5.29 (s, 2H, –N***H***$_2$Py); 6.15 (s, 4H, –NC***H***$_2$C$_6$H$_5$); 6.43 (d, 1H, J = 8.2 Hz, C***H***Py); 6.56 (d, 1H, J = 6.3 Hz, C***H***Py); 6.98–7.56 (m, 15H, Ar–***H*** and C***H***Py); 8.24 (d, 1H, J = 4.8 Hz, C***H***Py). ^{13}C NMR (100 MHz, $CDCl_3$) δ; 53.6 (–N***C***H$_2$C$_6$H$_5$); 111.3, 111.5, 114.2, 123.2, 128.1, 128.3, 128.7, 129.0, 134.8, 135.0 and 138.6 (Ar–***C***); 149.4 (***C***-Py); 158.1 (Pd-***C***$_{carbene}$).

2.3.5. Synthesis of the dibromo[1,3-dibenzylbenzimidazol-2-ylidene] triphenylphosphine palladium(II), *5*

This known complex **5** [42] was prepared by mixing dibromo[1,3-dibenzylbenzimidazol-2-ylidene]pyridinepalladium(II) **2** (129 mg, 0.2 mmol) and triphenylphosphine (53 mg, 0.2 mmol) in chloroform (15 mL) at 25 °C for 6 h. Yield: 73% (91 mg); m.p.: 287–288 °C; $\nu_{(CN)}$: 1410 cm^{-1}.

2.3.6. Synthesis of the dibromo[1,3-dibenzylbenzimidazol-2-ylidene] morpholinepalladium(II), *6*

The complex ***6*** was synthesized by the same method as complex **4**. But, morpholine (18 mg, 0.2 mmol) was used instead of 2-aminopyridine as ligand. Yield: 70% (91 mg); m.p.: 237–238 °C; $\nu_{(CN)}$: 1410 cm^{-1}; $\nu_{(N-H)}$: 3305 cm^{-1}. Anal. Calc. for $C_{25}H_{27}Br_2N_3OPd$: C: 46.07; H: 4.18; N: 6.45. Found: C: 46.25; H: 4.11; N: 6.32. ^{1}H NMR (400 MHz, $CDCl_3$); δ 2.73 (s, 1H, –N***H***(C***H***$_2$C***H***$_2$)$_2$O); 2.90 (t, 2H, J = 8.9 Hz, –NH(C***H***$_2$C***H***$_2$)$_2$O); 3.42 (m, 4H, –NH(C***H***$_2$C***H***$_2$)$_2$O); 3.74 (d, 2H, J = 8.5 Hz, –NH(C***H***$_2$C***H***$_2$)$_2$O); 6.00 (s, 4H, -NC***H***$_2$C$_6$H$_5$); 6.96–7.48 (m, 14H, Ar–***H***). ^{13}C NMR (100 MHz, $CDCl_3$) δ; 48.3 (–NH(***C***H$_2$CH$_2$)$_2$O); 53.6 (-N***C***H$_2$C$_6$H$_5$); 68.1 (–NH(CH$_2$***C***H$_2$)$_2$O); 111.5, 123.2, 128.0, 128.3, 128.9, 134.7 and 134.9 (Ar–***C***); 149.4 (***C***–Py); 165.9 (Pd–***C***$_{carbene}$).

2.4. Crystallography

Single crystal x-ray diffraction data of the complexes **3**, **4**, and **6** were obtained from a Rigaku Oxford XCalibur diffractometer including EOS CCD detector using MoK_α radiation with the operation condition of 50 kV and 40 mA (λ = 0.7107 Å) at 25 °C. CrysAlis^{Pro} software package was carried out for the data collections, cell refinements, data reductions and absorption corrections [43]. To perform structure solution and refinement process for each complex, the methods of SHELXT [44] and SHELXL [45] were applied, respectively via OLEX2 software [46]. All of the non-hydrogen atoms were processed as an anisotropic thermal ellipsoid. The riding model was used for determination of hydrogen atoms' positions. Crystallographic data of the all complexes were demonstrated in Table 1.

2.5. Biochemical studies

2.5.1. hCA isoenzymes activity assay

In this study, both hCA isoenzymes were obtained from expired waste blood human red blood cells using Sepharose-4B-L-Tyrosine-sulfanilamide affinity (SBLTS) chromatography [47] as described priorly [48], which was used as an affinity matrix for selective purification of hCA isoenzymes [49]. Our institution has approved the use of expired blood samples in our experimental studies. Both hCA isoenzymes activity was spectrophotometrically recorded according to Verpoorte et al. [50] and detailed in prior studies [51]. p-Nitrophenylacetate (PNA) was used as substrate for enzymatic reaction [52]. One CA isoenzyme unit is defined as the CA amount that had absorbance change at 348 nm of PNA to p-nitrophenolate ions (PNP) over a period of 3 min at 25 °C [53]. The quantity of protein during the purification procedure was determined according to prior study [54]. Bovine serum albumin was used as a standard protein [55, 56]. Discontinuous sodium dodecyl sulfate-polyacrylamide gel electrophoresis (SDS-PAGE) was used for screening of purity of both isoenzymes [57].

2.5.2. Acetylcholinesterase (AChE) activity assay

Acetylcholinesterase (from *Electrophorus electricus*) was obtained from Sigma-Aldrich. The effects of benzimidazolium salt **1**, palladium-based

Table 2. Selected bond parameters of the complexes.

Bond Lengths (Å)					
Complex 3		Complex 4		Complex 6	
Pd1–Br1	2.430 (14)	Pd1–Br1	2.4217 (7)	Pd1–Br1	2.4155 (7)
Pd1–Br2	2.4063 (19)	Pd1–Br2	2.4122 (7)	Pd1–Br2	2.4306 (7)
Cl1–C11	1.706 (17)	Pd1–N1	2.096 (4)	O1–C23	1.412 (6)
N2–C7	1.355 (16)	Pd1–C1	1.960 (4)	O1–C24	1.397 (6)
N3–C13	1.417 (17)	N2–C20	1.462 (6)	N2–C1	1.355 (4)
N1–C8	1.315 (15)	N3–C13	1.450 (6)	N3–C2	1.399 (4)
N2–C20	1.487 (17)	N4–C12	1.330 (7)	N2–C7	1.396 (4)
Pd1–N1	2.116 (10)	N2–C1	1.349 (6)	N3–C8	1.460 (5)
N1–C12	1.319 (18)	N1–C12	1.340 (6)	Pd1–N1	2.136 (3)
N3–C1	1.328 (17)	N3–C7	1.394 (6)	N1–C22	1.475 (5)
Pd1–C1	1.969 (12)	N2–C2	1.403 (6)	N2–C15	1.472 (4)
N2–C1	1.358 (17)	N1–C8	1.349 (7)	Pd1–C1	1.959 (3)
N3–C2	1.401 (16)	C20–C21	1.494 (7)	N3–C1	1.351 (4)
Bond Angeles (°)					
Br1–Pd1–Br2	176.24 (7)	Br1–Pd1–Br2	173.49 (3)	Br1–Pd1–Br2	175.59 (2)
Br2–Pd1–N1	89.9 (3)	Br2–Pd1–N1	92.02 (10)	Br2–Pd1–N1	92.68 (8)
Pd1–N1–C8	120.8 (9)	Pd1–N1–C8	118.1 (3)	C23–O1–C24	109.2 (3)
C1–N2–C7	116.1 (5)	Br1–Pd1–N1	90.79 (10)	C7–N2–C15	125.4 (3)
C1–N3–C2	108.4 (11)	Br2–Pd1–C1	88.60 (13)	C2–N3–C8	124.0 (3)
Pd1–N1–N2	124.0 (9)	Pd1–N1–C12	124.0 (3)	Br1–Pd1–N1	90.18 (18)
N3–C2–C3	128.2 (12)	Br1–Pd1–C1	88.46 (13)	Br2–Pd1–C1	88.93 (4)
Br1–Pd1–N1	92.4 (3)	N1–Pd1–C1	178.63 (17)	Pd1–N1–C22	120.3 (2)
Br2–Pd1–C1	88.7 (4)	C8–N1–C12	117.9 (4)	Pd1–C1–N2	129.6 (2)
Pd1–N1–C12	121.8 (8)	Pd1–C1–N2	127.1 (3)	Pd1–C1–N3	123.3 (2)
Br1–Pd1–C1	89.2 (4)	Pd1–C1–N3	125.5 (3)	Br1–Pd1–C1	88.65 (9)
N1–Pd1–C1	176.3 (5)	C1–N2–C20	124.5 (4)	N1–Pd1–C1	172.69 (12)
Pd1–C1–N3	128.5 (10)	C1–N3–C13	125.0 (4)	Pd1–N1–C25	106.2 (3)

complexes (**2**–**6**) and reference compounds including tacrine and donepezil on AChE activity were performed according to Ellman's method [58] as given previously [59]. The hydrolysis of acetylcholine iodide (AChI) by AChE was recorded at 412. Briefly, an aliquot (0.1 mL) of Tris/HCl buffer (1.0 M, pH 8.0) and different concentration of the synthesized benzimidazolium salt **1** and palladium-based complexes (**2**–**6**) were added to 50 μL of AChE enzyme solution (5.32×10^{-3} EU) and incubated for 10 min at 25 °C. Then, 50 μL of 5,5′-dithio-bis(2-nitro-benzoic) acid (DTNB) (0.5 mM) was added. The reaction was allowed to be initiated upon addition of 50 mL of AChI. The hydrolysis of AChI was monitored spectrophotometrically by the formation of the yellow 5-thio-2-nitrobenzoate anion, as a result of the reaction of DTNB with thiocholine, which released by enzymatic hydrolysis of AChI with maximum absorption at 412 nm [60].

2.5.3. Inhibition kinetic studies

To investigate the *in vitro* inhibition mechanism of the benzimidazolium salt **1** and palladium-based complexes (**2**–**6**), kinetic studies were realized with the different concentrations of benzimidazolium salt **1**, palladium-based complexes (**2**–**6**), and substrate. IC_{50} values and dawning of Lineweaver-Burk curves [61] were calculated as given previously [62, 63]. From the observed data, IC_{50} and K_i values for benzimidazolium salt **1** and palladium-based complexes (**2**–**6**) were computed, and the types of inhibition of both isoenzymes were evaluated as in previous study [64]. The lower IC_{50} shows the higher inhibition effects and the easier it is to use. The IC_{50} value is the most practical way for evaluation of inhibition affinities [65].

3. Results and discussion

3.1. Synthesis

The synthetic route for Pd(II)NHC complexes containing 1,3-dibenzylbenzimidazolium ligands **2–5** has been defined. The PEPPSI type Pd(II)NHC complexes **2** and **3** were prepared by mixing 1,3-dibenzylbenzimidazolium chloride [41], palladium chloride ($PdCl_2$), potassium bromide (KBr) and potassium carbonate (K_2CO_3) in pyridine/3-chloropyridine (4 mL) at 80 °C for 24 h (Scheme 1). All complexes in this study were obtained in good yields between 68 and 76%. All complexes dissolve well both in polar halogenated solvents such as chloroform and dichloromethane and in polar organic solvents such as dimethylformamide and dimethyl sulfoxide. In addition, other complexes containing morpholine and 2-amino ligands were less soluble both in polar organic solvents including ethyl alcohol and diethyl ether and in polar inorganic solvents including water, while complexes containing triphenylphosphine, pyridine, and 3-chloropyridine ligands were insoluble in these solvents. All complexes were insoluble in non-polar solvents including pentane, toluene and hexane. Finally, all complexes (**2**–**6**) remain stable in the solvent environment for a long time due to the stable metal-ligand bonds when dissolved in the solvent.

3.2. NMR study

The structures of all complexes were fully characterized by using ^1H NMR, ^{13}C NMR and, FTIR spectroscopic methods and elemental analysis

Table 3. Interactions geometry for the molecules (Å, °).

Nonclassical Hydrogen Bonds						
Complex	D–H•••A	D–H	H•••A	D•••A	D–H•••A	Symmetry code
3	C8–H8··· Br2	0.93	2.90	3.332 (13)	110	x,y,z
	C25–H25··· Br3	0.93	2.89	3.798 (18)	167	1 + x, −1 + y,z
4	N4–H4B··· Br2	0.86	2.76	3.553 (4)	154	1 − x, −y,1 − z
	C20–H20··· N4	0.97	2.58	3.394 (7)	141	1 − x,1 − y,1 − z
6	N1–H1··· Br1	0.98	2.84	3.229 (3)	104	x,y,z
	C8–H8A··· O1	0.97	2.48	3.381 (5)	154	1 − x,1/2 + y,1/2 − z
	C22–H22A··· Br2	0.97	2.89	3.522 (4)	124	x,y,z
X−Y···π Interactions						
	X–Y•••Cg	**Y•••Cg**	**X–Y•••Cg**	**X•••Cg**	**X–Y···π**	**Symmetry code**
4	C10–H10•••Cg5	2.74	152	3.591 (6)	56	1 − x, −y, 1 − z
	C19–H19•••Cg4	2.83	166	3.734 (6)	87	1/2 − x,1/2 + y,3/2 − z
	Pd–Br1•••Cg2	3.882 (2)	165.53 (4)	6.256 (2)	81.52	x,1 + y,z
	Pd–Br2•••Cg1	3.885 (2)	155.88 (4)	6.166 (2)	87.29	x, −1 + y,z
	Pd–Br2•••Cg3	3.438 (2)	170.50 (4)	5.831 (2)	84.96	x, −1 + y,z
6	C23–H23A•••Cg3	3.859 (5)	157	3.859 (5)	157	1/2 + x,1 − y,z

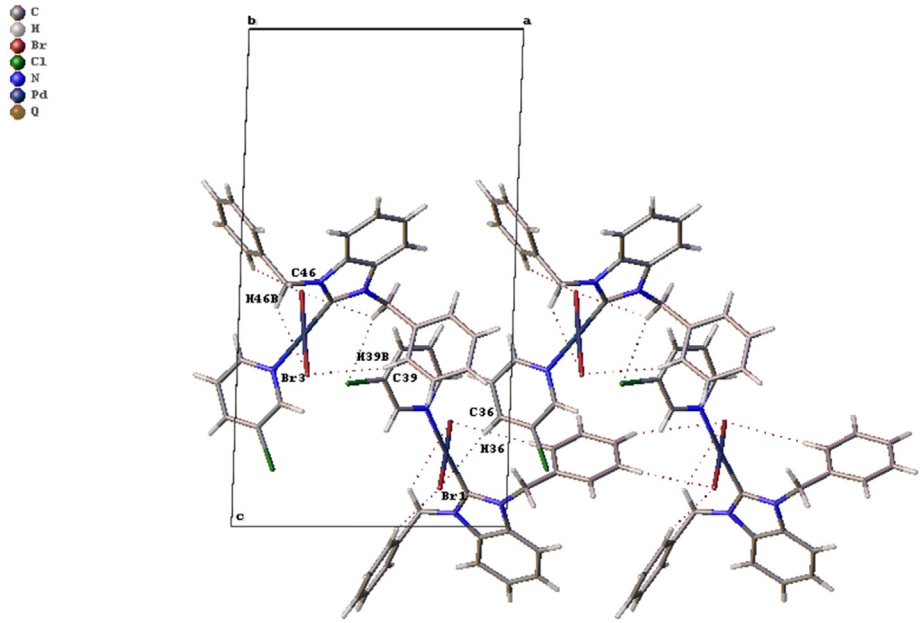

Figure 2. The packing arrangements of the complex 3 along the *010* plane.

technique. All data of these spectra were fully consistent with the proposed formula. For the ^{1}H NMR spectra, the data given below were observed. The acidic proton peak of the starting material (1,3-dibenzylbenzimidazolium chloride) [41] observed around 12.5 ppm was not observed in the spectra of the new the PEPPSI type Pd(II)NHC complexes **2** and **3**. Furthermore, characteristic proton peaks of the pyridine/3-chloropyridine ligand were showed between 8.88 and 9.00 ppm. However, the pyridine proton peaks that it observed between 8.88 and 9.00 ppm in the starting complex (**2**) were not observed in the ^{1}H NMR spectra of the other complexes (**4**–**6**). The amino (NH_2) protons in the 2-aminopyridine group for complex **4** were observed at 5.29 ppm as singlets. The amino (NH) proton in the morpholine group for complex **6** was observed at 2.73 ppm as singlets. Also, the CH_2 protons in the morpholine group for complex **6** were observed at 2.90, 3.42, and 3.74 ppm as triplet, multiplet, and doublet, respectively [18]. The significant increase in the number of aromatic protons between 7.00 and 8.00 ppm proves the presence of the triphenylphosphine group in the structure of complex **5**. Benzylic CH_2 protons were observed as singles around 6.00 ppm for complexes **2**–**4**, complex **6**, and as doublet at 4.78 ppm for complex **5**. For the ^{13}C NMR spectra, the data mentioned below were observed. The carbon peak of the starting material (1,3-dibenzylbenzimidazolium chloride) [41] observed around 143 ppm was not observed in the ^{13}C NMR spectra of the new PEPPSI type Pd(II)NHC complexes **2** and **3**. Furthermore, characteristic carbon peaks of the pyridine/3-chloropyridine ligand were observed between 150 and 152 ppm. However, the pyridine carbon peaks that it observed between 150 and 152 ppm in the starting complex (**2**) were not observed in the ^{13}C NMR spectra of the other complexes (**4**–**6**). The significant increase in the number of aromatic carbons between 123 and 135 ppm proves the presence of the triphenylphosphine group in the structure of complex **5** [12]. Benzylic CH_2 carbons were observed at around 54 ppm for all complexes (**2**–**6**). The carbons in the morpholine group for complex **6** were observed at 48.3 (C–N) and 68.1 (C–O) ppm [18]. The characteristic carbene peaks (2-$C_{carbene}$) were observed 163.2, 163.3, 158.1, 165.9, and

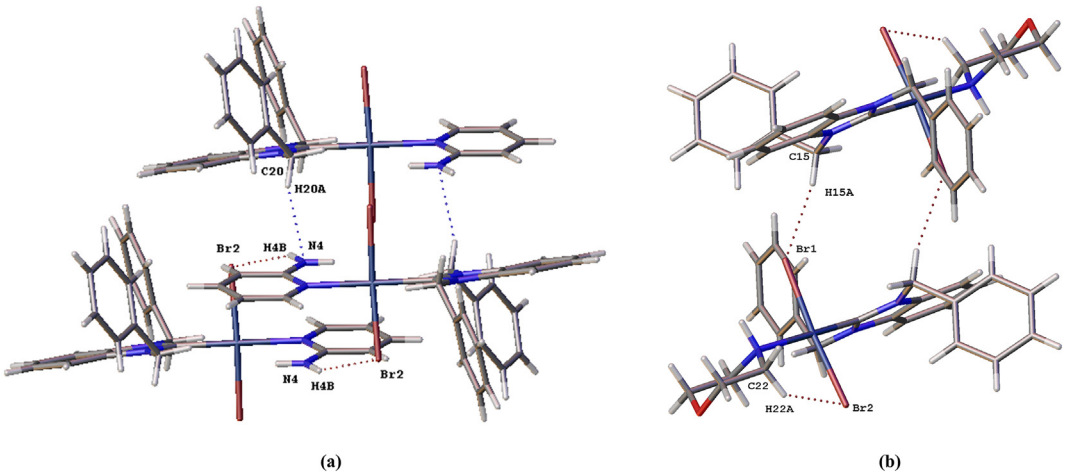

Figure 3. The view of the center-symmetric dimers of molecule complex **4** (a) and **6** (b) along the *(010)* plane.

176.7 ppm for all complexes **2–6**, respectively. Finally, the presence of a phosphorus peak at 26 ppm in the ^{31}P NMR spectrum for complex **5** proves that the triphenylphosphine ligand is coordinated to the palladium metal.

3.3. FTIR study

The FTIR spectra, the data given below were observed. The C–N stretching frequency observed at 1557 cm^{-1} for starting material (1,3-dibenzylbenzimidazolium chloride) [41] were observed around 1410 cm^{-1} for all complexes **2–6**. The N–H (primer) stretching frequency for the amino group in complex **4** was observed at 3325 and 3448 cm^{-1}. The N–H (seconder) stretching frequency for the morpholine group in complex **6** was observed at 3305 cm^{-1}. The C–O stretching frequency for the morpholine group in complex **6** was observed at 1027 cm^{-1}. The P-C_{Ar} stretching frequency for the triphenylphosphine group in complex **5** was observed at 1094 cm^{-1}. Also, it was shown that the calculated and experimentally determined elemental analysis were found to be very close to each other.

3.4. Structural details of the complexes

Heteroatom and functional group incorporation to the molecule backbone is highly effective in tuning the molecular structures, non-covalent interactions including non-classical hydrogen bonds, π···π stacking interactions, C − H···π, halogen ···π, and short interactions and their packing arrangements. Therefore, in the light of the data obtained from single crystal X-ray crystallography, the noticeable discrepancy was seen in the 3D molecular solid-state structures of the complexes and their packing arrangements created by the noncovalent interactions due to this reason. The molecular structures of the complexes were given in Figure 1. The crystallographic details including the bond lengths and angles of the complexes which are in good agreement with the similar structures reported in the literature were listed in Table 2 [66]. The crystallographic results revealed that complex **3** crystallizes in the triclinic space group P-1 with the two molecules in the asymmetric unit while the complex **6** and complex **4** crystallize in the monoclinic crystal system with space group I2/a and $P2_1/n$, respectively.

The 3D molecular structure of the trans-Pd (II) complexes (**3**, **4**, and **6**) demonstrated a slightly *distorted square planar* geometry with the palladium (II) center coordinated through the nitrogen (N1) atom which is the morpholine nitrogen atom and the pyridine nitrogen atom for the molecules **3** and **4** and a carbene carbon atom (C1) of the NHC ligand via two bromine atoms (Br1 and Br2). The bond angles around the Pd atoms (N1–Pd1–Br1: 92.4(3), 90.18(18), 90.79(10); N1–Pd1–Br2: 89.9(3)° 92.68(8) °, 92.02(10) °; C1–Pd1–Br1:89.2(4) °, 88.65(9) °, 88.46(13) °; C1–Pd1–Br2: 88.7(4) °, 88.93(4) °, 88.60(13) ° for all complexes) are very close to 90 ° due to the *distorted square planar* structures of coordination of the platinum (II) metal as reported for similar N-heterocyclic carbene complexes [67, 68] (Table 2). The coordination planes $PdBr_2CN$ of the complex **3**, **4,** and **6** are essentially planar to the molecule plane, with an overall r. m.s. deviation of 0.017 Å, 0.057 Å, and 0.034 Å, respectively.

The dihedral angles between the NHC and [PdBr2CN] mean planes are 109.98 (2)°, 92.259° and 94.824 (9)° for **3**, **4**, and **6**, respectively, while those between the pyridine and [PdBr2CN] mean planes are 142.123° and 105.67 (1)° for **3** and **4**, respectively and between the morpholine and [PdBr2CN] mean planes is 106.769 (2)° for **6**. This significant difference is likely due to van der Waals packing contacts raised from different functional groups with the ligands of neighboring complex molecules. The Pd-Carbene bond lengths of the complexes are an average of 1.962 Å are slightly shorter than the sum of the covalent radii of the associated atoms (dcov: Pd–C = 2.07 Å) since it has greater σ donating ability than that of usual NHC complexes [69]. The Pd − Br bond lengths which have an average of 2.42Å are between the expected values compared to the N-heterocyclic carbene palladium complexes. Additionally, Pd–N bond lengths (2.116(10) Å, 2.096(4) Å, and 2.136 (3) Å, for **3**, **4**, and **6** respectively) are consistent with reported similar trans-Pd (II) complexes, it is longer than the sum of individual covalent radii of Pd and N (1.983 Å), which is due to a strong trans effect of the NHC ligand residing diagonally opposite to the pyridine and morpholine rings [69, 70]. The morpholine ring of the complex **6** has a near chair conformation with puckering parameters q2: 0.554 (5), theta: 172.3 (4)°, and phi:174 .4 (4)° parameters.

The crystal packing of the Pd-based NHC complexes is determined by noncovalent intermolecular interactions, which also have significant effects on their biological activity results. Therefore, to further understand the biological activity of the studied complexes, their non-covalent interactions and packing structures in solid-phase were examined from the single-crystal X-ray crystallography data. The molecules **3** and **4** have chloropyridine and aminopyridine ligands, respectively that they can affect the geometry of the complex (bond lengths, angles, isomerism of the complex molecule). Interplay between intramolecular hydrogen bonding and the molecular geometry of the complex molecule has attracted great attention to obtain favorability of binding of ligands onto coordinatively unsaturated metal centers. Since a ligand's ability to form hydrogen bonds with other ligands can have an important effect on coordination geometries. Incorporation of neutral ligands to the complex molecule such as pyridine and amino pyridine which have excellent neutral Lewis bases coordinating to metal ions creates additional hydrogen bonding in the primary coordination sphere, therefore they have used in several examples of coordination chemistry [71,72]. The

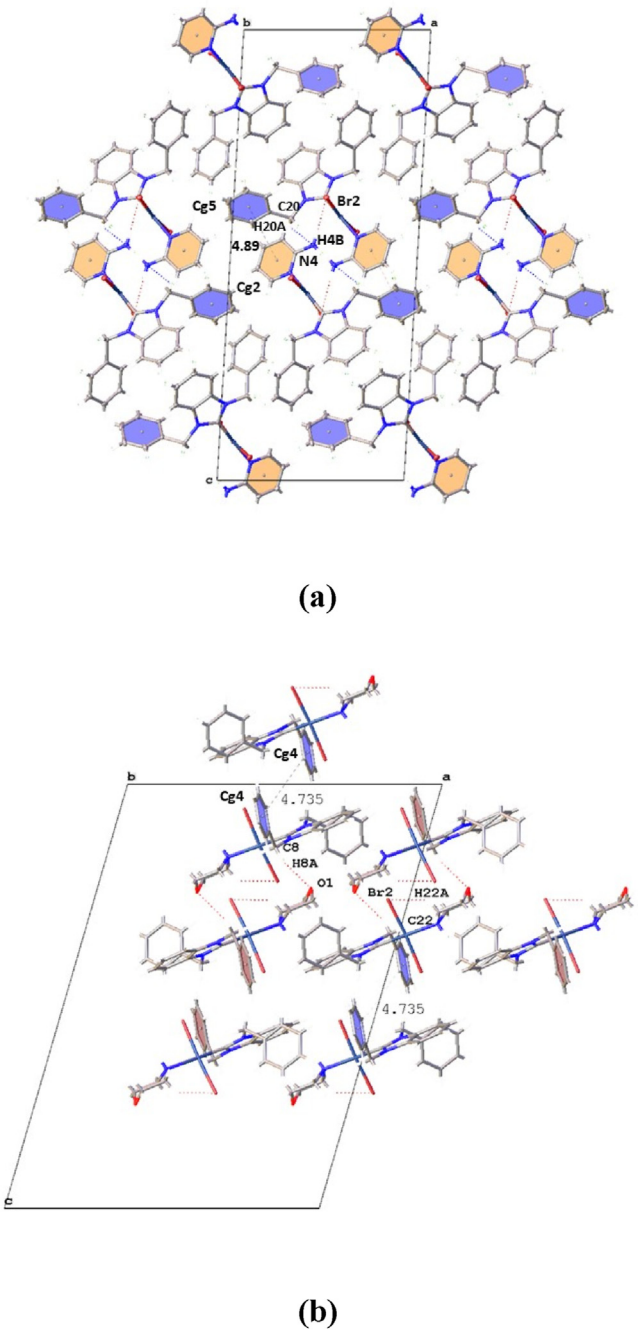

Figure 4. The packing arrangements of the complex **4** (a) and **6** (b) along the (010) plane.

aminopyridine ligand of the molecule **4** creates strong intermolecular hydrogen bond to the bromine atoms of the chelate plane and C20 carbon atom bounded to imidazole ring (N4–H4B··· Br2; C20–H20*A*··· N4) with change of the molecular packing of the complex. In addition, the presence of the weak intramolecular hydrogen bonding (C8– H8··· Br2) in the molecule **3** result in a lengthening of the Pd1–N1 [Pd1–N1: 2.116 Å for molecule **3** and 2.096 Å for molecule **4**) distance, as the intramolecular hydrogen bond draws the pyridine molecule away from the metal atom. When the a NH_2 substituent is present on the pyridine ring, the configuration of the molecule changes which allows the aminopyridine ligands to penetrate deeper into the coordination sphere as can be seen by the significant shortening of the Pd1–N1 [2.096 Å] bond distance. The dihedral angle between the phenyl and chelate rings (pyridine and [$PdBr_2CN$] mean planes are 142.123° and 105.67 (1)° for **3** and **4**, respectively and between the morpholine and [PdBr2CN] mean plane is 106.769 (2)° for **6**) and planarization of the complexes were affected by the type of the ligands. Morpholine ligand increase the planarity of the molecules which changes their molecular arrangements in solid phase.

According to crystallographic results, the molecular arrangements of the complex **3** is dominated by the nonclassical hydrogen bonds (C8–H8··· Br2 and C25–H25··· Br3) and short interactions (Br1–H36 (2.99 Å) intermolecular short interactions and Br3–H46 (2.69 Å) intramolecular short interactions) while the hydrogen bonds, π···π stacking interactions, C – H···π, halogen ···π interactions are responsible for the molecular arrangements of the complex **4** (Table 3). The molecular packing arrangement of complex **3** is given in Figure 2.

Due to the strong intermolecular interactions of the molecule **4** allow the formation of strong π ··· π stacking interactions (Cg5 ··· Cg2: 4.895 Å; Cg2:N1–C8/C12; Cg5:C21/C26) and dimeric structure since adjacent molecules in solid phase approaches each other thanks to electrostatic interactions in crystal phase. Beside the π ··· π stacking interactions, unlike the molecule **3**, C – H···π and Pd – Br···π interactions were observed in crystal structure of the molecule **4**. These interactions enhance the rigidity and stability of the molecule **4** in its molecular arrangements.

Introducing an morpholine ring to the complex leads to formation of intramolecular hydrogen bonds (N1–H1··· Br1; C22–H22A··· Br2) which cause to distortion of the coordination geometry and extension of the Pd1–N1 bonds (2.136 (3) Å), as compared to the other molecules. Similar shortening of the Pd–N bond length when the morpholine ring is present have been observed the previous studies. The presence of the intramolecular H-bonding in the crystal structure of the complex which are molecules **3** and **6** enable the extension of the Pd1–N1 bonds since the H atoms attracts the ligands from the Pd metal ion. This situation is similar to previous studies given in the literature [73, 74]. In addition, due to the presence of the electron acceptor O atom which influence electron distribution in the molecule, molecule **6** has strong intermolecular hydrogen bonding (C8–H8A··· O1) for generation of the C–H•••π (C23–H23A•••Cg3; Cg3: C2/C7) and intermolecular π •••π stacking interactions (Cg4 ··· Cg4:4.735 Å ; Cg4:C9/C14).

The complexes **4** and **6** displayed supramolecular dimer by their intermolecular interactions (C20 – H20*A*··· N4 and N4– H4B··· Br2 hydrogen bonds for complex **4**, Br1 ··· H15A short interactions between the neighboring molecules) leading to centre-symmetric R_2^2 (15) and R_2^2 (12) graphset motifs, respectively (Figure 3). These dimeric structures of the complexes enhance their structural rigidity in the solid phases of the molecules **4** and **6**.

The packing in the crystal structures of the complexes **4** and **6** is achieved by the intermolecular π ··· π stacking interactions (Cg4 ··· Cg4:4.735 Å for complex **6** and Cg5 ··· Cg2: 4.895 Å for the complex **4**; Cg2:N1–C8/C12; Cg4:C9/C14; Cg5:C21/C26), nonclassical intra and intermolecular hydrogen bonds (N4–H4B··· Br2 and C20–H20*A*··· N4 hydrogen bonds for complex **4** and C8 – H8··· O1 and C22 – H22*A*··· Br2 for complex **6**) along the *(010)* plane (Table 3; Figure 4).

3.5. Enzyme inhibition results

Recently, many compounds associated with enzyme inhibition have been evaluated to improve human health and demonstrate the health importance of inhibitors [75, 76, 77]. The synthesized benzimidazolium salt **1** and a series of novel the Palladium-based complexes bearing 1, 3-dibenzylbenzimidazolium with morpholine, triphenylphosphine, and pyridine derivate ligands, (**2**–**6**), were tested towards cytosolic isoforms hCA I, hCA II and AChE.

1. All the novel synthesized complexes effectively inhibited cytosolic hCA I isoenzyme with IC_{50}s ranging from 31.5 to 115.5 nM. IC_{50} value of an inhibitor is the required concentration to inhibit half of the

Table 4. Inhibition parameters of AChE and hCA I, II with the benzimidazolium salt **1** and palladium-based complexes bearing 1,3-dibenzylbenzimidazolium with morpholine, triphenylphosphine, and pyridine derivate ligands (**2–6**).

Compounds	IC_{50} (nM)						K_i (nM)		
	hCA I	r^2	hCA II	r^2	AChE	r^2	hCA I	hCA II	AChE
1	115.5	0.9760	69.3	0.9863	86.6	0.9951	68.5 ± 11.5	49.3 ± 6.5	64.1 ± 9.0
2	46.2	0.9813	21.0	0.9820	26.6	0.9940	28.4 ± 1.2	8.3 ± 1.8	22.8 ± 3.2
3	31.5	0.9907	16.1	0.9774	21.6	0.9982	10.0 ± 1.4	7.7 ± 0.6	24.5 ± 2.9
4	53.3	0.9847	30.1	0.9985	43.3	0.9736	18.1 ± 3.0	19.7 ± 1.9	38.6 ± 5.0
5	36.4	0.9984	19.2	0.9875	27.7	0.9847	40.3 ± 2.0	15.3 ± 4.2	23.1 ± 2.6
6	35.1	0.9955	13.3	0.9816	25.6	0.9714	16.9 ± 0.3	12.1 ± 1.4	32.1 ± 3.2
AZA	68.1	0.9803	39.6	0.9811	-	-	52.1 ± 4.2	27.4 ± 3.1	-
TAC	-	-	-	-	42.9	0.9889	-	-	40.2 ± 2.1
Donepezil	-	-	-	-	37.4	0.9902			34.1 ± 2.2

maximum enzyme activity [78]. Also, K_i values varies in ranging of 10.0 ± 1.4–68.5 ± 11.5 nM. Also, the studied complexes exhibited the best inhibition effects when compared to AZA (K_i: 52.1 ± 4.2 nM). Among them, the complex of dibromo [1,3-dibenzylbenzimidazol-2-ylidene]-3-chloropyridinepalladium (II) (**3**) demonstrated the best inhibition (K_i: 10.0 ± 1.4 nM). The inhibition effects of benzimidazolium salt **1** and palladium-based complexes bearing 1,3-dibenzylbenzimidazolium with morpholine, triphenylphosphine, and pyridine derivate ligands (**2–6**) on hCA I were decreased as follows: **3** (K_i: 10.0 ± 1.4 nM) > **6** (K_i: 16.9 ± 0.3 nM) > **4** (K_i: 18.1 ± 3.0 nM) > **2** (K_i: 28.4 ± 1.2 nM) > **5** (K_i: 40.3 ± 2.0 nM) > **1** (K_i: 68.5 ± 11.5 nM) (Table 4). According to results, chlorine binding to the 3rd position of the benzene ring of complex **2** increased the 2.83-fold inhibition, binding amino group 2nd position of the benzene ring increased the 2.83 times inhibition.

2. Also, the benzimidazolium salts bearing chloro-/fluorobenzyl-substituted compounds inhibited hCA II with IC_{50}s between 13.33-69.30 nM and K_is ranging from 7.7 ± 0.6 to 49.3 ± 6.5 nM. The inhibition effects of benzimidazolium salt **1** and palladium-based complexes bearing 1,3-dibenzylbenzimidazolium with morpholine, triphenylphosphine, and pyridine derivate ligands (**2–6**) towards hCA II were decreased in the following order: **3** (K_i: 7.7 ± 0.6 nM) > **2** (K_i: 8.3 ± 1.8 nM) > **6** (K_i: 12.0 ± 1.4 nM) > **5** (K_i: 15.0 ± 4.2 nM) > **4** (K_i: 19.7 ± 1.9 nM) > **1** (K_i: 49.3 ± 6.5 nM) (Table 4). Similar to hCA I, the complex **3** showed the best inhibition effect toward hCA II isoenzyme. Otherwise, the morpholine group showed more effective inhibition than the amino group unlike hCA I.
3. All of the synthesized Palladium-based complexes bearing 1,3-dibenzylbenzimidazolium ligands exhibited an efficient inhibition effect on AChE with IC_{50}s between 21.6-86.6 nM and K_is between 22.8 ± 3.2–64.0 ± 9.0 nM. Herein, unlike both hCA isoenzymes, complex **2** demonstrated the highest inhibition with K_i constant of 22.8 ± 3.2 nM, 1.76-fold more effective inhibition than tacrine (K_i: 40.2 ± 2.1 nM) and 1.49-fold donepezil (K_i: 34.1 ± 2.2 nM). The inhibition properties of benzimidazolium salt **1** and palladium-based complexes bearing 1,3-dibenzylbenzimidazolium with morpholine, triphenylphosphine and pyridine derivate ligands (**2–6**) against AChE were decreased in the following order: **2** (K_i: 22.8 ± 3.2 nM) > **5** (K_i: 23.1 ± 2.6 nM) > **3** (K_i: 24.5 ± 2.9 nM) > **6** (K_i: 32.1 ± 3.2 nM) > **4** (K_i: 38.6 ± 5.0 nM) > **1** (K_i: 64.0 ± 9.0 nM) (Table 4). When compounds **3** and **4** are evaluated, the binding of chlorine group instead of the amino group linked to the aromatic benzene ring caused an increased inhibition ability. Looking at the results, inhibition values for compounds **2**, **3** and **4** for the AChE enzyme are close to each other.

4. Conclusions

As a result, four new Pd(II)NHC complexes were reported in this work. All complexes' structures were fully characterized by using spectroscopic methods (^{1}H NMR, ^{13}C NMR and FTIR) and elemental analysis technique. The existence of Pd-carbene peaks in the expected region in ^{13}C NMR shows that the structure was consistent with the proposed formula. A single peak observed in the ^{31}P NMR spectrum proves that PPh_3 coordinates to the Pd center. The C–N stretching vibrations in the FTIR spectrum prove that the NHC ligand is coordinated to the Pd center. N–H stretches of primary and secondary amines demonstrate that the ligand of 2-aminopyridine and morpholine are coordinated to the Pd center, respectively. The crystal structures of three complexes were determined. According to crystallographic results, incorporation to aminopyridine ligand leads to generation of intermolecular hydrogen bonding which result in different packing arrangements, molecular geometry and stability in the solid phase of the complex molecule. Morpholine ring in the complex enable to formation of intramolecular hydrogen bonds, which cause to distortion of the coordination geometry and extension of the Pd1–N1 bonds, as compared to the other molecules. As a briefly, the presence of the intramolecular H-bonding in the crystal structure of the complex result in the extension of the Pd1–N1 bonds Due to change in the molecular conformation with the different ligands form differences in the molecular arrangements and number and type of the inter-intermolecular interactions therefore it allows to increase stability and rigidity of the crystal structure in solid phase. The enzyme inhibition activities of benzimidazolium salt **1** and palladium-based complexes bearing 1,3-dibenzylbenzimidazolium with morpholine, triphenylphosphine, and pyridine derivate ligands (**2–6**) were examined against AChE and hCAs I and II isoforms, which associated with some common and global diseases including AD, epilepsy and glaucoma.

Declarations

Author contribution statement

Aydın Aktaş: Performed the experiments; Wrote the paper.

Gül Yakal, Yeliz Demir: Performed the experiments.

İlhami Gülçin: Conceived and designed the experiments; Contributed reagents, materials, analysis tools or data; Wrote the paper.

Muhittin Aygün: Analyzed and interpreted the data; Wrote the paper.

Yetkin Gök: Conceived and designed the experiments; Analyzed and interpreted the data; Contributed reagents, materials, analysis tools or data.

Funding statement

This work was supported by the Dokuz Eylül University for the use of the Oxford Rigaku Xcalibur Eos Diffractometer (purchased under University Research Grant No: 2010.KB.FEN.13).

Data availability statement

Data associated with this study has been deposited at Crystallographic data as.cif files for the structures reported in this paper have been

deposited at the Cambridge Crystallographic Data Center under the accession number CCDC 2103176 for 3, 2102940 for 4, and 2102939 for 6.

Declaration of interests statement

The authors declare no conflict of interest.

Additional information

Supplementary content related to this article has been published online at https://doi.org/10.1016/j.heliyon.2022.e10625.

References

[1] R.D.J. Froese, C. Lombardi, M. Pompeo, R.P. Rucker, M.G. Organ, Designing Pd–N-heterocyclic carbene complexes for high reactivity and selectivity for cross-coupling applications, Acc. Chem. Res. 50 (2017) 2244–2253.

[2] D. Janssen-Müller, C. Schlepphorst, F. Glorius, Privileged chiral N-heterocyclic carbene ligands for asymmetric transition-metal catalysis, Chem. Soc. Rev. 46 (2017) 4845–4854.

[3] K. Azouzi, C. Duhayon, I. Benaissa, N. Lugan, Y. Canac, S. Bastin, V. Cesar, Bidentate iminophosphorane-NHC ligand derived from the imidazo [1,5-a] pyridin-3-ylidene scaffold, Organometallics 37 (2018) 4726–4735.

[4] V. Karthik, V. Gupta, G. Anantharaman, Synthesis, structure, and coordination chemistry of phosphine-functionalized imidazole/imidazolium salts and cleavage of a C–P Bond in an NHC–phosphenium salt using a Pd(0) precursor, Organometallics 34 (2015) 3713–3720.

[5] P.G. Edwards, F.E. Hahn, Synthesis and coordination chemistry of macrocyclic ligands featuring NHC donor groups, Dalton Trans 40 (2011) 10278–10288.

[6] M. Richert, M. Walczyk, M.J. Cieslak, J. Kazmierczak-Baranska, K. Krolewska-Golinska, G. Wrzeszcz, T. Muziol, S. Biniak. Synthesis, X-ray structure, physicochemical properties and anticancer activity of mer and fac Ru(III) triphenylphosphine complexes with a benzothiazole derivative as a co-ligand, Dalton Trans 48 (2019) 10689–10702.

[7] B.K. Keppler, W. Rupp, Antitumor activity of imidazolium-bisimidazole-tetrachlororuthenate (III). A representative of a new class of inorganic antitumor agents, J. Cancer Res. Clin. Oncol. 111 (1986) 166–168.

[8] F.T. Garzon, M.R. Berger, B.K. Keppler, D. Schmahl, Comparative antitumor activity of ruthenium derivatives with 5′-deoxy-5-fluorouridine in chemically induced colorectal tumors in SD rats, Cancer Chemother, Pharmacology 19 (1987) 347–349.

[9] E. Alessio, L. Messori, Metallo-Drugs: Development and Action of Anticancer Agents, in: A. Sigel, H. Sigel, E. Freisinger, R.K.O. Sigel (Eds.), MetalIons in Life Sciences, first ed. 18, Walter de Gruyter GmbH, Berlin, Germany, 2018, pp. 141–170.

[10] C.J. O'Brien, E.A.B. Kantchev, C. Valente, N. Hadei, G.A. Chass, A. Lough, A.C. Hopkinson, M.G. Organ, An all-purpose Pd-NHC precatalyst for cross-coupling reactions, Chem. Eur J. 12 (2006) 4743–4748.

[11] J.F. Lua, J. Zhaoa, Sunb Ming, X.H. Jia, Huanga Pei, H.G. Ge, Synthesis and crystal structure of 1-(3-amino-4-morpholino-1h-indazole-1-carbonyl)-n-(4-methoxyphenyl) cyclopropane-1-carboxamide, a molecule with antiproliferative activity, Crystallogr. Rep. 66 (2021) 455–460.

[12] F. Erdemir, D. Barut Celepci, A. Aktaş, Y. Gök, New (NHC) Pd (II)(PPh_3) complexes: synthesis, characterization, crystal structure and its application on Sonogashira and Mizoroki–Heck cross-coupling reactions, Chem. Pap. 74 (2020) 99–112.

[13] S. Bal, Ö. Demirci, B. Şen, P. Taslimi, A. Aktaş, Y. Gök, M. Aygün, İ. Gulçin, PEPPSI type Pd(II)NHC complexes bearing chloro-/fluorobenzyl group: synthesis, characterization, crystal structures, α-glycosidase and acetylcholinesterase inhibitory properties, Polyhedron 198 (2021) 115060.

[14] S. Dasgin, Y. Gok, D. Barut Celepci, P. Taslimi, M. İzmirli, A. Aktaş, I. Gulcin, Synthesis, characterization, crystal structure and bioactivity properties of the benzimidazole-functionalized PEPPSI type of Pd (II) NHC complexes, J. Mol. Struct. 1228 (2021) 129442.

[15] F. Türker, S.A.A. Noma, A. Aktaş, K. Al-Khafaji, T. Taşkın Tok, B. Ateş, Y. Gök, The (NHC)$PdBr_2$(2-aminopyridine) complexes: synthesis, characterization, molecular docking study, and inhibitor effects on the human serum carbonic anhydrase and serum bovine xanthine oxidase, Monatsh. Chem. 151 (2020) 1557–1567.

[16] F. Erdemir, D. Barut Celepci, A. Aktaş, Y. Gök, R. Kaya, P. Taslimi, Y. Demir, I. Gulcin, Novel 2-aminopyridine liganded Pd (II) N-heterocyclic carbene complexes: synthesis, characterization, crystal structure and bioactivity properties, Bioorg. Chem. 91 (2019) 103134.

[17] M. Hyeraci, M. Colalillo, L. Labella, F. Marchetti, S. Samaritani, V. Scalcon, M.P. Rigobello, L.D. Via, Platinum (II) complexes bearing triphenylphosphine and chelating oximes: antiproliferative effect and biological profile in resistant cells, ChemMedChem 15 (2020) 1464–1472.

[18] F. Türker, C. Gürses, D. Barut Celepci, A. Aktaş, B. Ateş, Y. Gök, New morpholine-liganded palladium (II) N-heterocyclic carbene complexes: synthesis, characterization, crystal structure, and DNA-binding studies, Arch. Pharm. 352 (12) (2019) 1900187.

[19] M. Yigit, D. Barut Celepci, P. Taslimi, B. Yigit, B. Çetinkaya, İ. Özdemir, M. Aygün, İ. Gulçin, Selenourea and thiourea derivatives of chiral and achiral enetetramines: synthesis, characterization and enzyme inhibitory properties, Bioorg. Chem. 120 (2022) 105566.

[20] D. Aktaş Anıl, M.F. Polat, R. Sağlamtas, A.H. Tarikoğulları, M.A. Alagöz, İ. Gülçin, O. Algül, S. Burmaoğlu, Exploring enzyme inhibition profiles of novel halogenated chalcone derivatives on some metabolic enzymes: synthesis, characterization and molecular modeling studies, Comput. Biol. Chem. 100 (2022) 107748.

[21] O. Hisar, Ş. Beydemir, I. Gulcin, Ö.İ. Küfrevioğlu, C.T. Supuran, Effects of low molecular weight plasma inhibitors of rainbow trout (*Oncorhynchus mykiss*) on human erythrocyte carbonic anhydrase-II isozyme activity *in vitro* and rat erythrocytes in vivo, J. Enzyme Inhib. Med. Chem. 20 (2005) 35–39.

[22] A. Scozzafava, P. Kalın, C.T. Supuran, I. Gulcin, S. Alwasel, The impact of hydroquinone on acetylcholine esterase and certain human carbonic anhydrase isoenzymes (hCA I, II, IX, and XII), J. Enzyme Inhib. Med. Chem. 30 (6) (2015) 941–946.

[23] C. Caglayan, P. Taslimi, C. Türk, F.M. Kandemir, Y. Demir, I. Gulcin, Purification and characterization of the carbonic anhydrase enzyme from horse mackerel (*Trachurus trachurus*) muscle and the impact of some metal ions and pesticides on enzyme activity, Comp. Biochem. Physiol. Part C 226 (2019) 108605.

[24] A. Sujayev, E. Garibov, P. Taslimi, I. Gulcin, S. Gojayeva, V. Farzaliyev, S.H. Alwasel, C.T. Supuran, Synthesis of some tetrahydropyrimidine-5-carboxylates, determination of their metal chelating effects and inhibition profiles against acetylcholinesterase, butyrylcholinesterase and carbonic anhydrase, J. Enzyme Inhib. Med. Chem. 31 (6) (2016) 1531–1539.

[25] B. Kuzu, M. Tan, I. Gulcin, N. Menges, A novel class for carbonic anhydrases inhibitors and evaluation of their non-zinc binding, Arch. Pharm. 354 (10) (2021) e2100188.

[26] M. Küçük, İ. Gulcin, Purification and characterization of the carbonic anhydrase enzyme from Black Sea trout (*Salmo trutta* Labrax Coruhensis) kidney and inhibition effects of some metal ions on enzyme activity, Environ. Toxicol. Pharmacol. 44 (2016) 134–139.

[27] F. Topal, K. Aksu, I. Gulcin, F. Tümer, Tohma, S. Göksu, Inhibition profiles of some symmetric sulfamides derived from phenethylamines on human carbonic anhydrase I, and II isoenzymes, Chem. Biodivers. 18 (10) (2021) e2100422.

[28] C. Çağlayan, Y. Demir, S. Küçükler, P. Taslimi, F.M. Kandemir, I. Gulcin, The effects of hesperidin on sodium arsenite-induced different organ toxicity in rats on metabolic enzymes as antidiabetic and anticholinergics potentials: a biochemical approach, J. Food Biochem. 43 (2) (2019) e12720.

[29] C. Caglayan, P. Taslimi, Y. Demir, S. Küçükler, M.F. Kandemir, I. Gulcin, The effects of zingerone against vancomycin-induced lung, liver, kidney and testis toxicity in rats: the behavior of some metabolic enzymes, J. Biochem. Mol. Toxicol. 33 (10) (2019) e22381.

[30] F. Ozbey, P. Taslimi, I. Gulcin, A. Maraş, S. Goksu, C.T. Supuran, Synthesis of diaryl ethers with acetylcholinesterase, butyrylcholinesterase and carbonic anhydrase inhibitory actions, J. Enzyme Inhib. Med. Chem. 31 (S2) (2016) 79–85.

[31] M. Nar, Y. Çetinkaya, I. Gulcin, A. Menzek, (3,4-Dihydroxyphenyl)(2,3,4-trihydroxyphenyl) methanone and its derivatives as carbonic anhydrase isoenzymes inhibitors, J. Enzyme Inhib. Med. Chem. 28 (2) (2013) 402–406.

[32] F. Turkan, A. Cetin, P. Taslimi, M. Karaman, I. Gulcin, Synthesis, biological evaluation and molecular docking of novel pyrazole derivatives as potent carbonic anhydrase and acetylcholinesterase inhibitors, Bioorg. Chem. 86 (2019) 420–427.

[33] B. Özgeriş, S. Göksu, L. Köse Polat, I. Gulcin, R.E. Salmas, S. Durdagi, F. Tümer, C.T. Supuran, Acetylcholinesterase and carbonic anhydrase inhibitory properties of novel urea and sulfamide derivatives incorporating dopaminergic 2-aminotetralin scaffolds, Bioorg. Med. Chem. 24 (10) (2016) 2318–2329.

[34] Y. Demir, P. Taslimi, M.S. Ozaslan, N. Oztaskın, Y. Çetinkaya, I. Gulcin, S. Beydemir, P. Göksu, Antidiabetic potential: *In vitro* inhibition effects of bromophenol and diarylmethanones derivatives on metabolic enzymes, Arch. Pharm. 351 (12) (2018) e1800263.

[35] F. Erdemir, D. Barut Celepci, A. Aktaş, P. Taslimi, Y. Gök, H. Karabıyık, I. Gulcin, 2-Hydroxyethyl substituted NHC precursors: synthesis, characterization, crystal structure and carbonic anhydrase, α-glycosidase, butyrylcholinesterase, and acetylcholinesterase inhibitory properties, J. Mol. Struct. 1155 (2018) 797–806.

[36] D. Ozmen Ozgün, H.İ. Gül, C. Yamali, H. Sakagami, I. Gulcin, M. Sukuroglu, C.T. Supuran, Synthesis and bioactivities of pyrazoline benzensulfonamides as carbonic anhydrase and acetylcholinesterase inhibitors with low cytotoxicity, Bioorg. Chem. 84 (2019) 511–517.

[37] C. Yamali, H.İ. Gül, Y. Demir, C. Kazaz, I. Gulcin, Synthesis and bioactivities of 1-(4-hydroxyphenyl)-2-((heteroaryl) thio) ethanones as carbonic anhydrase I, II and acetylcholinesterase inhibitors, Turk. J. Chem. 44 (2020) 1058–1067.

[38] Ç. Bayrak, P. Taslimi, H.S. Kahraman, I. Gulcin, A. Menzek, The first synthesis, carbonic anhydrase inhibition and anticholinergic activities of some bromophenol derivatives with S including natural products, Bioorg. Chem. 85 (2019) 128–139.

[39] E. Garibov, P. Taslimi, A. Sujayev, Z. Bingöl, S. Çetinkaya, I. Gulcin, S. Beydemir, V. Farzaliyev, S.H. Alwasel, C.T. Supuran, Synthesis of 4,5-disubstituted-2-thioxo-1,2,3,4-tetrahydropyrimidines and investigation of their acetylcholinesterase, butyrylcholinesterase, carbonic anhydrase I/II inhibitory and antioxidant activities, J. Enzyme Inhib. Med. Chem. 31 (S3) (2016) 1–9.

[40] İ. Gulcin, A. Scozzafava, C.T. Supuran, H. Akıncıoğlu, Z. Koksal, F. Turkan, S. Alwasel, The effect of caffeic acid phenethyl ester (CAPE) on metabolic enzymes including acetylcholinesterase, butyrylcholinesterase, glutathione S-transferase, lactoperoxidase, and carbonic anhydrase isoenzymes I, II, IX, and XII, J. Enzyme Inhib. Med. Chem. 31 (6) (2016) 1095–1101.

[41] P.V. Thong, N. Hien, N.S. Ha, N.T.T. Chi, Synthesis and structure of some azolium salts, Vietnam J. Chem 55 (2) (2017) 249–254.

[42] S.K. Yen, L.L. Koh, H.V. Huynh, T.S. Andy Hor, Structures and Suzuki-coupling of N-heterocyclic carbene complexes of PdII with coordinated solvent and PPh_3, Aust. J. Chem. 62 (2009) 1047–1053.

[43] Agilent Technologies, CrysAlis PRO and CrysAlis RED, Yarnton, Oxfordshire England, 2002.

[44] G.M. Sheldrick, SHELXT-Integrated space-group and crystal-structure determination, Acta Crystallogr. A 71 (2015) 3–8.

[45] G.M. Sheldrick, Crystal structure refinement with SHELXL, Acta Crystallogr. C 71 (2015) 3–8.

[46] O.V. Dolomanov, L.J. Bourhis, R.J. Gildea, J.A.K. Howard, H. Puschmann, OLEX2: a complete structure solution, refinement and analysis program, J. Appl. Crystallogr. 42 (2009) 339–341.

[47] O. Arslan, B. Nalbantoglu, N. Demir, H. Özdemir, Ö.I. Küfrevioglu, A new method for the purification of carbonic anhydrase isozymes by affinity chromatography, Tr. J. Med. Sci. 26 (1996) 163–166.

[48] P. Taslimi, I. Gulcin, N. Öztaşkın, Y. Çetinkaya, S. Göksu, S.H. Alwasel, C.T. Supuran, The effects of some bromophenols on human carbonic anhydrase isoenzymes, J. Enzyme Inhib. Med. Chem. 31 (4) (2016) 603–607.

[49] U.M. Koçyiğit, Y. Budak, M.B. Gürdere, F. Ertürk, B. Yencilek, P. Taslimi, I. Gulcin, M. Ceylan, Synthesis of chalcone-imide derivatives and investigation of their anticancer and antimicrobial activities, carbonic anhydrase and acetylcholinesterase enzymes inhibition profiles, Arch. Physiol. Biochem. 124 (2018) 61–68.

[50] J. Verpoorte, A. Mehta, S. Edsall, Esterase activities of human carbonic anhydrases B and C, J. Biol. Chem. 242 (18) (1967) 4221–4229.

[51] M. Huseynova, P. Taslimi, A. Medjidov, V. Farzaliyev, M. Aliyeva, G. Gondolova, O. Şahin, B. Yalçın, A. Sujayev, E.B. Orman, A.R. Özkaya, I. Gulcin, Synthesis, characterization, crystal structure, electrochemical studies and biological evaluation of metal complexes with thiosemicarbazone of glyoxylic acid, Polyhedron 155 (2018) 25–33.

[52] A. Kazancı, Y. Gok, R. Kaya, A. Aktaş, P. Taslimi, I. Gulcin, Synthesis, characterization and bioactivities of dative donor ligand N-heterocyclic carbene (NHC) precursors and their Ag (I) NHC coordination compounds, Polyhedron 193 (2021) 114866.

[53] C. Yamali, H.İ. Gül, A. Ece, P. Taslimi, I. Gulcin, Synthesis, molecular modeling, and biological evaluation of 4-[5-aryl-3-(thiophen-2-yl)-4,5-dihydro-1H-pyrazol-1-yl] benzenesulfonamides toward acetylcholinesterase, carbonic anhydrase I and II enzymes, Chem. Biol. Drug Des. 91 (4) (2018) 854–866.

[54] E. Köksal, İ. Gülçin, Purification and characterization of peroxidase from cauliflower (*Brassica oleracea* L.) buds, Protein Pept. Lett. 15 (4) (2008) 320–326.

[55] A. Biçer, P. Taslimi, G. Yakali, I. Gulcin, M.S. Gültekin, G. Turgut Cin, Synthesis, characterization, crystal structure of novel bis-thiomethylcyclohexanone derivatives and their inhibitory properties against some metabolic enzymes, Bioorg. Chem. 82 (2019) 393–404.

[56] H. Goksu, M. Topal, A. Keskin, M.S. Gültekin, M. Çelik, I. Gulcin, M. Tanc, C.T. Supuran, 9,10-Dibromo-N-aryl-9,10-dihydro-9,10-[3,4]epipyrroloanthracene-12,14-diones: synthesis and investigation of their effects on carbonic anhydrase isozymes I, II, IX, and XII, Arch. Pharm. 349 (6) (2016) 466–474.

[57] P. Taslimi, C. Caglayan, I. Gulcin, The impact of some natural phenolic compounds on carbonic anhydrase, acetylcholinesterase, butyrylcholinesterase, and α-glycosidase enzymes: an antidiabetic, anticholinergic, and antiepileptic study, J. Biochem. Mol. Toxicol. 31 (12) (2017) e21995.

[58] G.L. Ellman, K.D. Courtney, V. Andres, R.M. Jr, Feather-Stone, A new and rapid colorimetric determination of acetylcholinesterase activity, Biochem. Pharmacol. 7 (1961) 88–95.

[59] S. Burmaoğlu, A.O. Yılmaz, M.F. Polat, R. Kaya, İ. Gülçin, Ö. Algül, Synthesis and biological evaluation of novel tris-chalcones as potent carbonic anhydrase, acetylcholinesterase, butyrylcholinesterase, and α-glycosidase inhibitors, Bioorg. Chem. 85 (2019) 191–197.

[60] M. Gumus, Ş.N. Babacan, Y. Demir, Y. Sert, İ. Koca, İ. Gulcin, Discovery of sulfadrug-pyrrole conjugates as carbonic anhydrase and acetylcholinesterase inhibitors, Arch. Pharm. 355 (2022) e2100242.

[61] H. Lineweaver, D. Burk, The determination of enzyme dissociation constants, J. Am. Chem. Soc. 56 (1934) 658–666.

[62] I. Mahmudov, Y. Demir, Y. Sert, Y. Abdullayev, E. Sujayev, S.H. Alwasel, I. Gulcin, Synthesis and inhibition profiles of N-benzyl-and N-allyl aniline derivatives against carbonic anhydrase and acetylcholinesterase-A molecular docking study, Arab. J. Chem. 15 (2022) 103645.

[63] S. Bilginer, B. Anıl, M. Koca, Y. Demir, I. Gulcin, Novel Mannich bases with strong carbonic anhydrases and acetylcholinesterase inhibition effects: 3-(aminomethyl)-6-{3-[4-(trifluoromethyl)phenyl]acryloyl}-2(3H)-benzoxazolones, Turk. J. Chem. 45 (2021) 805–818.

[64] B. Turan, K. Sendil, E. Sengul, M.S. Gultekin, P. Taslimi, I. Gulcin, C.T. Supuran, The synthesis of some β-lactams and investigation of their metal-chelating activity, carbonic anhydrase and acetylcholinesterase inhibition profiles, J. Enzyme Inhib. Med. Chem. 31 (S1) (2016) 79–88.

[65] I. Gulcin, S.H. Alwasel, Metal Ions, Metal chelators and metal chelating assay as antioxidant method, Processes 10 (2022) 132.

[66] E.V. Bermesheva, A.I. Wozniak, F.A. Andreyanov, G.O. Karpov, M.S. Nechaev, A.F. Asachenko, M.A. Topchiy, E.K. Melnikova, Y.V. Nelyubina, P.S. Gribanov, M.V. Bermeshev, Polymerization of 5-Alkylidene-2-norbornenes with highly active Pd–N-Heterocyclic carbene complex catalysts: catalyst structure–activity relationships, ACS Catal. 10 (2020) 1663–1678.

[67] S.S. Batsanov, Experimental Foundations of Structural Chemistry, Moscow University Press, Moscow, 2008, p. 542.

[68] M. Ibrahim, I. Malik, W. Mansour, M. Sharif, M. Fettouhi, B. El Ali, Novel (N-heterocyclic carbene)Pd(pyridine)Br2 complexes for carbonylative Sonogashira coupling reactions: catalytic efficiency and scope for arylalkynes, alkylalkynes and dialkynes, Appl. Organomet. Chem. 32 (2018) e4280.

[69] A. Aktaş, Barut Celepci, R. Kaya, P. Taslimi, Y. Gök, M. Aygün, I. Gulcin, Novel morpholine liganded Pd-based N-heterocyclic carbene complexes: synthesis, characterization, crystal structure, antidiabetic and anticholinergic properties, Polyhedron 159 (2019) 345–354.

[70] I. Cvrtila, V. Stilinovic, B. Kaitner, Tuning of coordination geometry via cooperation of inter- and intramolecular hydrogen bonds in bis(benzoylacetonato) manganese(II) adducts with pyridine derivatives, CrystEngComm 15 (2013) 6585–6593.

[71] I. Cvrtila, V. Stilinovic, B. Kaitner, Morpholine adducts of Co, Ni, and Mn benzoylacetonates: isostructurality and C–H…O hydrogen bonding, Struct. Chem. 23 (2012) 587–594.

[72] K. Gholivand, H. Mostaanzadeh, T. Koval, M. Dusek, M.F. Erben, H. Stoeckli-Evans, C.O.D. Vedova, Syntheses, spectroscopic study and X-ray crystallography of some new phosphoramidates and lanthanide(III) complexes of N-(4-nitrobenzoyl)- N',N''-bis(morpholino)phosphoric triamide, Acta Crystallogr. B 66 (2010) 441–450.

[73] F. Perdih, Diversity of supramolecular aggregation in copper(II) pentane-2,4-dionato compounds with methyl substituted 2-aminopyridines, J. Coord. Chem. 65 (2012) 1580–1591.

[74] N. Bedekovic, M. Cavka, D. Cincic, V. Stilinovic, Influence of intramolecular hydrogen bonding on structures and thermal stability of Cu(II) and Zn(II) β-diketonate adducts, J. Mol. Struct. 1246 (2021) 131130.

[75] H.I. Gul, E. Mete, P. Taslimi, I. Gulcin, C.T. Supuran, Synthesis, carbonic anhydrase I and II inhibition studies of the 1,3,5-trisubstituted-pyrazolines, J. Enzyme Inhib. Med. Chem. 32 (2017) 189–192.

[76] K. Küçükoğlu, H.İ. Gül, P. Taslimi, I. Gulcin, C.T. Supuran, Investigation of inhibitory properties of some hydrazone compounds on hCA I, hCA II and AChE enzymes, Bioorg. Chem. 86 (2019) 316–321.

[77] L. Durmaz, A. Ertürk, M. Akyüz, L. Polat Köse, E.M. Uc, Z. Bingöl, R. Sağlamtaş, S. Alwasel, I. Gulcin, Screening of carbonic anhydrase, acetylcholinesterase, butyrylcholinesterase and α-glycosidase enzymes inhibition effects and antioxidant activity of coumestrol, Molecules 27 (2022) 3091.

[78] S. Burmaoğlu, E.A. Kazancioglu, M.Z. Kazancioglu, R. Saglamtaş, G. Yalçın, I. Gulcin, O. Algül, Synthesis, molecular docking and some metabolic enzyme inhibition properties of biphenyl-substituted chalcone derivatives, J. Mol. Struct. 1254 (2022) 132358.